Accurate Non-Quasi-Static Gate-Source Impedance Model of RF MOSFETs

Hyun-Jun Lee and Seonghearn Lee

Abstract—**An improved non-quasi-static gate-source impedance model including a parallel RC block for short-channel MOSFETs is developed to simulate RF MOSFET input characteristics accurately in the wide range of high frequency. The non-quasi-static model parameters are accurately determined using the physical input equivalent circuit. This improved model results in much better agreements between the measured and modelled input impedance than a simple one with a non-quasi-static resistance up to 40GHz, verifying its accuracy.**

Index Terms—**MOSFET, CMOS, RF, model, non-quasi-static, parameter extraction**

I. INTRODUCTION

Physically, NQS(non-quasi-static) effect in MOSFETs is a relaxation-time dependent phenomenon of channel charge response by a time-varying input signal [1, 2]. The inversion channel region is distributed in the lateral direction under the gate oxide [3], and this distributed nature results in the channel propagation delay. This non-quasi-static effect due to the channel delay plays an important role in the high frequency region [4].

In order to model this delay effect, the channel region of the MOSFET is represented as an RC distributed network that is very complex for IC simulation [3]. In order to simplify this complexity, a simple small-signal MOSFET model with a single NQS gate-source resistance is widely used [3-11], but it is too simple to model the distributed channel effect in the wide range of high-frequency accurately.

In particular, it is important to develop the accurate gate-source impedance model in the high-frequency region because a gate resistance will have strong influence on the input impedance and increase the noise figure of the transistor.

Therefore, in this paper, we propose an improved NQS gate-source impedance model including a NQS parallel RC block to extend the valid frequency limit to 40GHz. We also present a new NQS gate-source impedance extraction method using the physical input equivalent circuit.

II. NQS MODELING AND PARAMETER EXTRACTION

S-parameters are measured on multi-finger N-MOSFETs (0.18 μm gate length, 16 gate finger and 5 μm unit finger width). An accurate de-embedding procedure was carried out to remove pad and interconnection parasitics from each measured S-parameters [12].

Fig. 1(a) shows a simple small-signal MOSFET model [11] with NQS gate-source resistance R_{gsi}. In this model, R_{ge} is the electrode gate resistance, C_{gsi} is the gate-source channel capacitance, C_{gso} is the overlap gate-source capacitance, C_{gd} is the gate-drain capacitance, R_d is the drain resistance, R_s is the source resistance, C_{jd} is the drain junction capacitance, R_{bk} is the bulk resistance, and C_{bk} is the bulk capacitance.

In order to know whether this simple model is

Manuscript received May. 10, 2013; accepted Oct. 5, 2013
A part of this work was presented in Korean Conference on Semiconductors, Gangwon-do in Korea, Feb. 2013.
Department of Electronic Engineering, Hankuk University of Foreign Studies, San 89, Wangsan-ri, Mohyun-myun, Yongin, Kyungki-do 449-791, Korea
E-mail : shlee@hufs.ac.kr

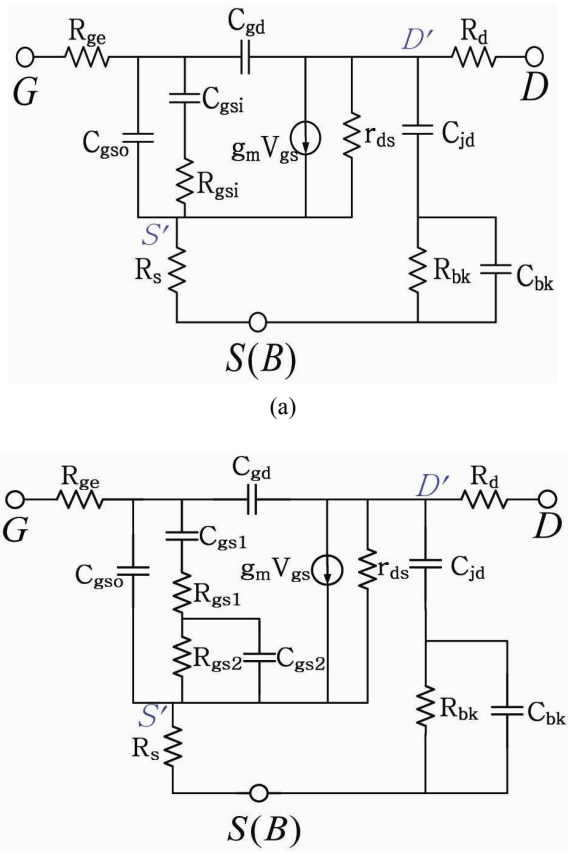

Fig. 1. Small-signal MOSFET equivalent circuit in the saturation region (a) Using simple NQS gate-source resistance model, (b) Using improved NQS gate-source impedance model.

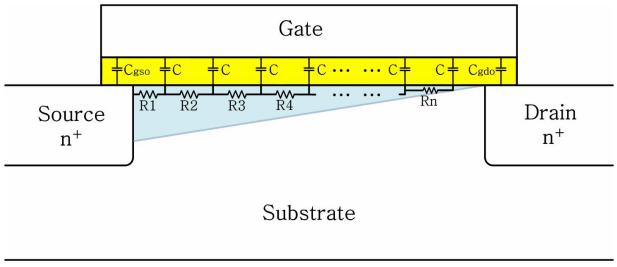

Fig. 2. Non-quasi-static RC distributed network to represent lateral channel of MOSFET in the saturation region.

physically valid, ac current flow in distributed gate oxide and channel region is investigated in detail. In Fig. 2, the inversion channel region in the saturation region is represented by n RC ladder network distributed in the lateral direction. The larger ac current will flow in unit oxide capacitance of $C = C_{ox}/n$ that is closer to the edge of source, because the larger voltage is applied across C closer to the source edge due to ac potential drop across the differential channel resistances R_2, R_3, ⋯ R_n in Fig. 2. This potential drop becomes larger at higher frequency, because the impedance of $1/(j\omega C)$ decreases. Therefore, the gate-to-source ac current tend to crowd around the source edge, as frequency becomes higher. Since this ac current crowding near the source edge results in shorter ac current path between gate and source, the equivalent resistance of R_{gsi} greatly decreases with increasing frequency.

This decreasing frequency-dependence of R_{gsi} can be physically represented as an impedance of parallel RC block. Thus, the simple model with a single resistance R_{gsi} in Fig. 1(a) is not physically acceptable.

In this paper, an improved small-signal MOSFET model with the additional NQS parallel block of resistance and capacitance (R_{gs2}, C_{gs2}) in Fig. 1(b) is proposed for better high-frequency modeling than Fig. 1(a).

Fig. 3 shows the physical input equivalent circuits

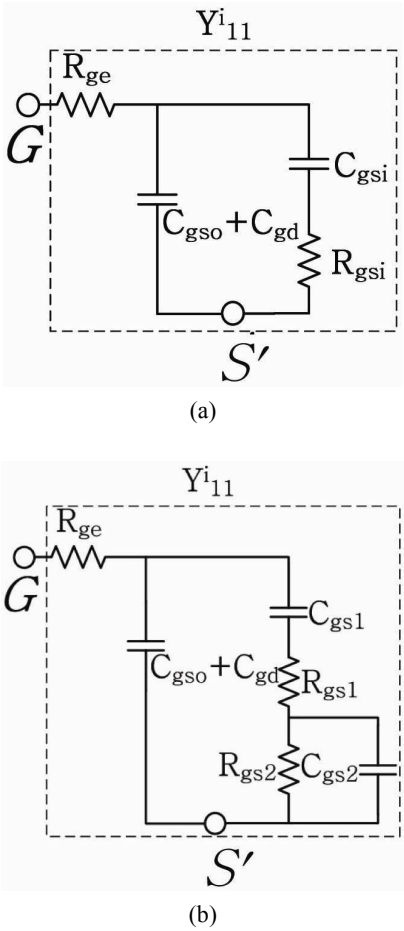

Fig. 3. Input equivalent circuit in the saturation region (a) For extraction method using simple NQS model, (b) For extraction method using improved NQS model.

defined by Y^i_{11}-parameter after R_d, C_{jd}, R_{bk}, C_{bk}, and R_s are removed from Fig. 1. In Fig. 3, C_{gd} is added to C_{gso} because Y^i_{11} is defined at shorted internal drain (D') and source (S').

In the simple model, R_{gsi} in Fig. 1(a) is extracted using the following equation [11] derived from input equivalent circuit of Fig. 3(a) in the low-frequency range of $\omega \ll 1/(R_gC_{gg})$ where $R_g = R_{gsi}+R_{ge}$ and $C_{gg} = C_{gso}+C_{gsi}+C_{gd}$:

$$\mathrm{Re}(Y^i_{11,LF})/[\mathrm{Im}(Y^i_{11,LF})]^2 \approx R_{ge} + k^2R_{gsi} \quad (1)$$

where $$k = C_{gsi}/(C_{gso} + C_{gd} + C_{gsi}) \quad (2)$$

After R_d, C_{jd}, R_{bk}, C_{bk}, and R_s are determined using a RF direct extraction method [13], Y^i_{11} is determined by subtracting them from measured S-parameters. Fig. 5 shows V_{gs}–dependence of $\mathrm{Re}(Y^i_{11,LF})/[\mathrm{Im}(Y^i_{11,LF})]^2$ determined by selecting average values of measured data at near 5 GHz in Fig. 4.

Since R_{ge} is independent of V_{gs}, R_{ge} is determined to be 1.6Ω by finding a lowest limited value of $\mathrm{Re}(Y^i_{11,LF})/[\mathrm{Im}(Y^i_{11,LF})]^2$ at infinite V_{gs} using a curve-fitting of Fig. 5.

In order to determine k in (2), C_{gso} is extracted to be 26fF using the following equation derived in accumulation region ($V_{gs} = V_{FB} = -1.5$V, $V_{ds} = 0$V), where V_{FB} is flat-band voltage [14]:

$$C_{gso} = C_{gdo} = -(1/\omega)\mathrm{Im}(Y^i_{12})_{LF} \quad (3)$$

where C_{gso} is assumed to be equal to C_{gdo} at $V_{ds} = 0$V for symmetric MOSFETs. The frequency dependent data of $-(1/\omega)\mathrm{Im}(Y^i_{12})$ in (3) are plotted and C_{gdo} is taken from the low frequency data in Fig. 6.

The value of C_{gd} is extracted using $-(1/\omega)\mathrm{Im}(Y^i_{12})_{LF}$ at $V_{ds} = 1$V. The C_{gsi} value is next extracted by $C_{gs} - C_{gso}$ where $C_{gs} = (1/\omega)\mathrm{Im}(Y^i_{11}+Y^i_{12})_{LF}$ at $V_{ds} = 1$V. The frequency dependent data of $-(1/\omega)\mathrm{Im}(Y^i_{12})$ and $(1/\omega)\mathrm{Im}(Y^i_{11}+Y^i_{12})$ in the saturation region are plotted with varying V_{gs} in Fig. 7. The V_{gs}-dependent data of C_{gsi} and C_{gd} extracted in the low frequency region are shown in Fig. 8. After k is calculated from (2) using C_{gso}, C_{gsi} and C_{gd}, V_{gs}-dependent data of R_{gsi} using the simple model are extracted by substituting k in (1). The extracted k increases with gate voltage due to the rise of C_{gsi}, as shown in Fig. 9. Using $\{\mathrm{Re}(Y^i_{11,LF})/[\mathrm{Im}(Y^i_{11,LF})]^2$ $- R_{ge}\}/k^2$ of (1), V_{gs}-dependent data of R_{gsi} for the simple model in Fig. 1(a) are extracted in Fig. 10.

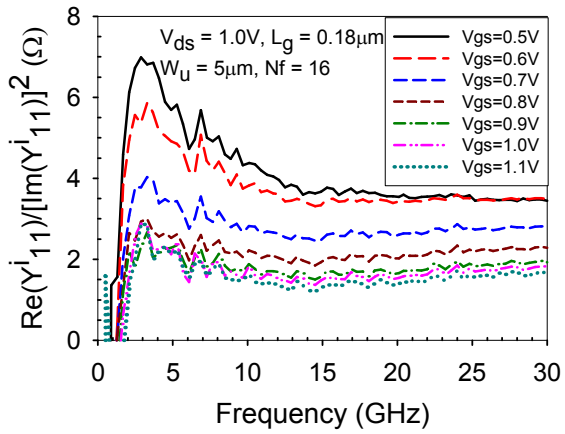

Fig. 4. Frequency response of $\mathrm{Re}(Y^i_{11})/[\mathrm{Im}(Y^i_{11})]^2$ at various V_{gs}.

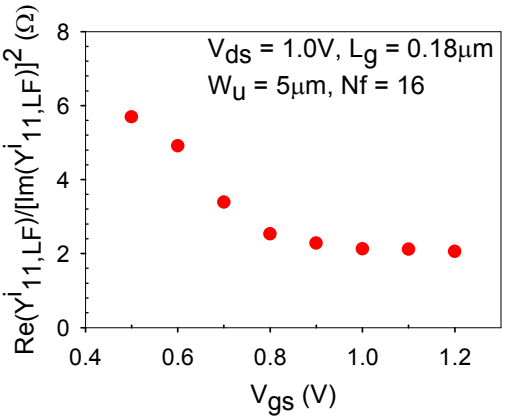

Fig. 5. Extracted $\mathrm{Re}(Y^i_{11,LF})/[\mathrm{Im}(Y^i_{11,LF})]^2$ versus V_{gs}.

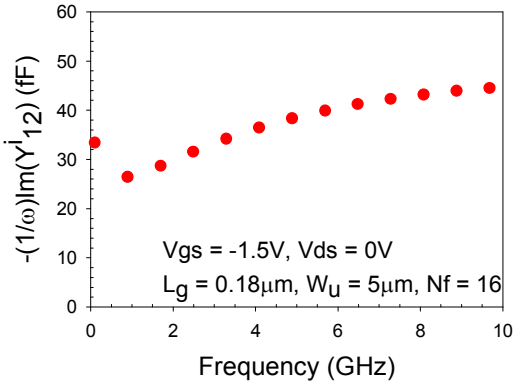

Fig. 6. Frequency dependent data of $-(1/\omega)\mathrm{Im}(Y^i_{12})$ in accumulation region.

However, simulated real term of input impedance $\mathrm{Real}(1/Y_{11})$ data for a simple NQS model of Fig. 1(a) with R_{gsi} extracted using (1) shows severe disagreement

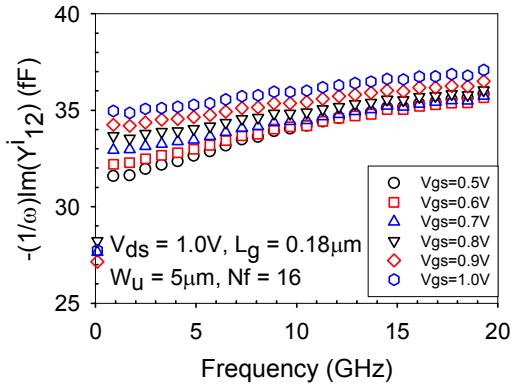

(a)

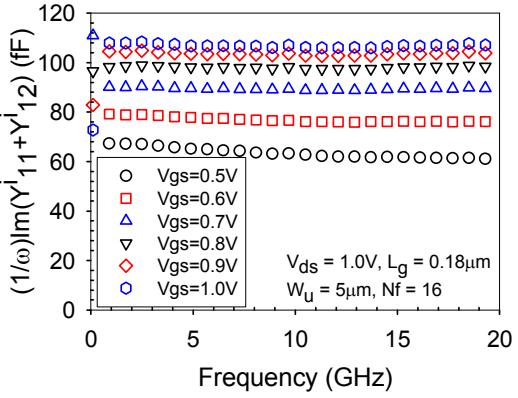

(b)

Fig. 7. Frequency dependent data in the saturation region (a) $-(1/\omega)\mathrm{Im}(Y^i_{12})$, (b) $(1/\omega)\mathrm{Im}(Y^i_{11}+Y^i_{12})$.

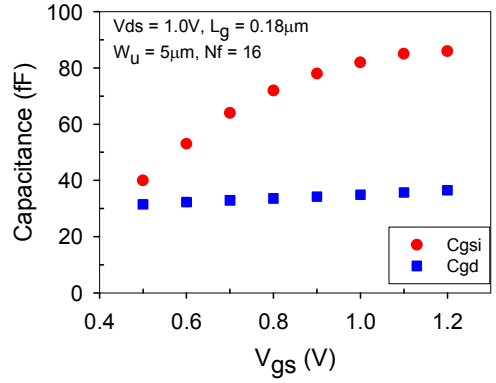

Fig. 8. V_{gs}-dependent data of extracted C_{gsi} and C_{gd}.

in the frequency region up to 40 GHz as shown in Fig. 12. In order to find out the cause of the disagreement, frequency-dependence has been analyzed as follows: The 3-dB cutoff frequency of $f_{cs} \approx 1/(2\pi R_g C_{gg})$ in a simple input equivalent circuit of Fig. 3(a) is estimated to be 234.8 GHz at V_{gs} = 0.6 V. Due to this very high

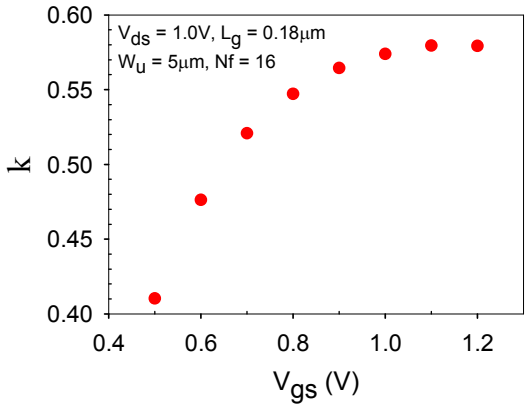

Fig. 9. Extracted k versus V_{gs}.

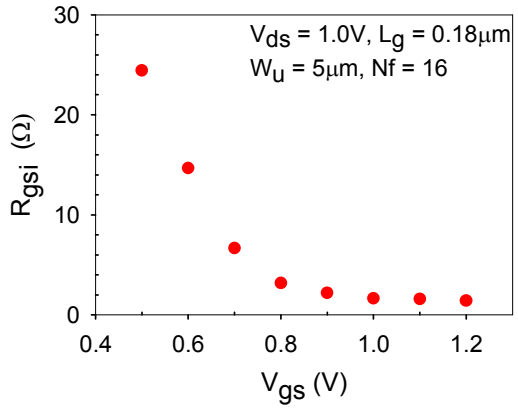

Fig. 10. Extracted NQS resistances versus V_{gs} for simple model.

frequency of f_{cs}, Real($1/Y_{11}$) of Fig. 1(a) becomes almost constant up to 40GHz as shown in Fig. 12. Thus, the simple NQS model can not simulate the decreasing frequency-dependence due to ac current crowding effect, resulting in large deviation from the measured data up to 40 GHz in Fig. 12.

In order to model the decreasing frequency dependency of Fig. 12, an improved NQS gate-source impedance model including the additional R_{gs2} and C_{gs2} block in Fig. 1(b) is proposed. The NQS model parameters are extracted using the following new method:

In the high-frequency(HF) range of $1/(R_{gs2}C_{gs2}) \ll \omega \ll 1/(R_g C_{gg})$, the following equation is approximated from Fig. 3(b) because the impedance of $R_{gs2} \parallel C_{gs2}$ is neglected:

$$\mathrm{Re}(Y^i_{11,HF})/[\mathrm{Im}(Y^i_{11,HF})]^2 \approx R_{ge} + k^2 R_{gs1} \qquad (4)$$

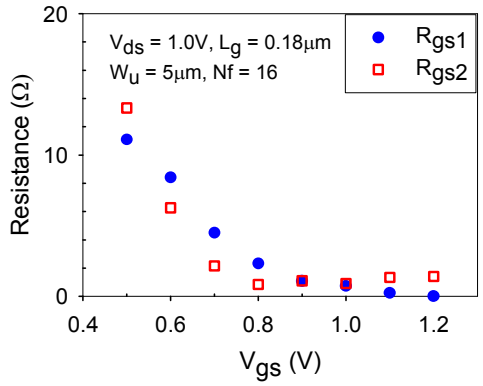

Fig. 11. Extracted NQS resistances versus V_{gs} for improved model.

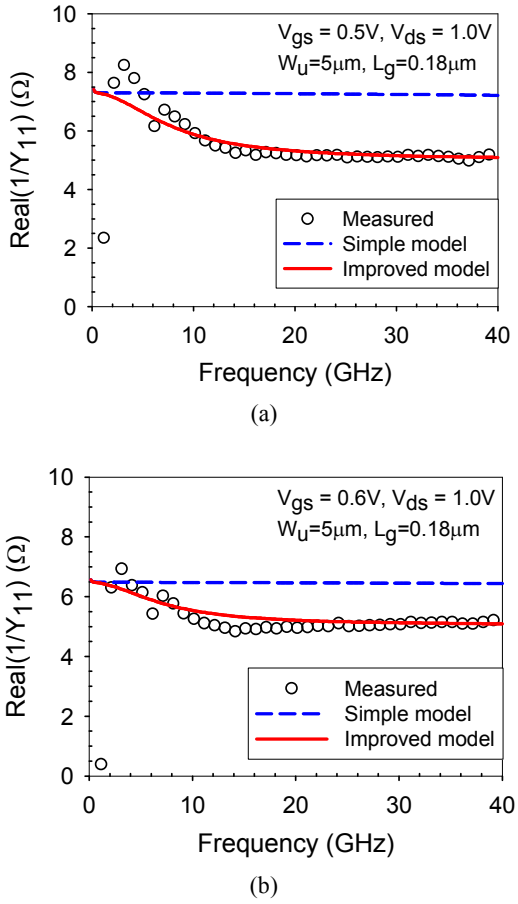

Fig. 12. Frequency response of Real($1/Y_{11}$) of simple and improved small-signal models (Fig. 1) compared with measured data (a) V_{gs}=0.5 V, (b) V_{gs}=0.6 V.

In the low-frequency range of $\omega \ll 1/(R_{gs2}C_{gs2})$, the following equation is approximated from Fig. 3(b):

$$\mathrm{Re}(Y^{i}_{11,LF})/[\mathrm{Im}(Y^{i}_{11,LF})]^2 \approx R_{ge} + k^2(R_{gs1}+R_{gs2}) \quad (5)$$

R_{gs1} and R_{gs2} are extracted by substituting the high and low frequency values of Fig. 4 in (4) and (5), respectively. The V_{gs}-dependent data of R_{gs1} and R_{gs2} extracted using the new method are shown in Fig. 11.

For C_{gs1} extraction, the following equation is used in the low-frequency range of $\omega \ll 1/(R_{gs2}C_{gs2})$:

$$C_{gs1} \approx (1/\omega)\mathrm{Im}(Y^{i}_{11}+Y^{i}_{12})_{LF} - C_{gso} \quad (6)$$

Using (6), it is found that C_{gs1} = 53fF at V_{gs} = 0.6 V. The value of C_{gs2} is extracted by fitting measured S-parameters up to 40 GHz.

Since the 3-dB cutoff frequency of $f_{ci} \approx 1/(2\pi R_{gs2}C_{gs2})$ = 7.3 GHz at V_{gs} = 0.6 V is calculated in a new input equivalent circuit of Fig. 3(b), the improved NQS model of Fig. 1(b) can accurately simulate the decreasing behavior due to ac current crowding effect in the input resistance of Real($1/Y_{11}$) up to 15 GHz of Fig. 12.

As shown in Fig. 12, the simulated real term of input impedance Real($1/Y_{11}$) data of the improved NQS MOSFET model of Fig. 1(b) show better agreement with measured one up to 40GHz than those of the simple one, verifying the accuracy of the improved model.

CONCLUSIONS

An improved non-quasi-static gate-source impedance model including an additional NQS parallel RC block is developed to predict MOSFET input characteristics accurately. Using the improved model, a frequency response of input impedance is well predicted in the high-frequency region. The accuracy of the improved model has been verified by observing the better agreement between the measured and modeled input resistance up to 40 GHz than the simple one.

ACKNOWLEDGMENTS

This research was supported by Basic Science Research Program through the National Research Foundation of Korea (NRF) funded by the Ministry of Education, Science and Technology (2010-0025549).

REFERENCES

[1] Y. Tsividis, *Operation and Modeling of the MOS*

Transistor, 2nd ed. New York: Oxford Univ. Press, 1999.

[2] X. Jin, K. Cao, J.-J. Ou, W. Liu, Y. Cheng, M. Matloubian, and C. Hu, "An accurate non-quasistatic MOSFET model for simulation of RF high speed circuits," *Proc. 2000 Symp. VLSI Technol. Dig. Tech. Papers*, June 2000.

[3] M. Chan., K.Y. Hui, C. Hu, and P.K. Ko, "A robust and physical BSIM3 non-quasi-static transient and AC small-signal model for circuit simulation," *IEEE Trans. Electron Devices*, vol. 45, no. 4, pp. 834-841, 1998.

[4] M. Bagheri and Y. Tsividis, "A small-signal DC-to-high-frequency nonquasistatic model for the four-terminal MOSFET valid in all regions of operation," *IEEE Trans. Electron Devices*, vol. ED-32, no. 11, pp. 2383-2391, 1985.

[5] P. J. V. Vandeloo, W. M. C. Sansen, "Modeling of the MOS transistor for high frequency analog design," *IEEE Trans Computer-Aided Design*, vol. 8, no. 7, pp. 713-723, 1989.

[6] C. E. Biber, M. L. Schmatz, T. Morf, U. Lott, W. Bachtold, "A nonlinear microwave MOSFET model for Spice simulators," *IEEE Trans. Microwave Theory Tech*., vol. 46, no. 5, pp. 604-610, 1998.

[7] J. P. Raskin, R. Gillon, J. Chen, D. Vanhoenacker-Janvier, J.-P. Colinge, "Accurate SOI MOSFET characterization at microwave frequencies for device performance optimization and analog modeling," *IEEE Trans Electron Devices*, vol. 45, no. 5, pp. 1017-1025, 1998.

[8] S. Lee and H. K. Yu, "Determining non-quasi-static small-signal equivalent circuit of a RF silicon MOSFET," *Solid State Electronics*, vol. 45, pp. 359-364, 2001.

[9] I. M. Kang and H. Shin, "Non-quasi-static small-signal modeling and analytical parameter extraction of SOI FinFETs", *IEEE Transaction on Nanotechnology*, vol. 5, no. 3, pp. 205-210, 2006.

[10] I. M. Kang, "Non-quasi-static RF model for SOI FinFET and its verification," *Journal of Semiconductor Technology and Science*, vol. 10, no. 2, pp.160-164, 2010.

[11] H.-J. Lee and S. Lee, "A new extraction method for non-quasi-static gate resistance of RF MOSFETs," *Electron. Lett*, vol. 48, no. 23, pp. 1501-1503, 2012.

[12] J.-Y. Kim, M.-K. Choi, and S. Lee, "A "thru-short-open" de-embedding method for accurate on-wafer RF measurements of nano-scale MOSFETs," *Journal of Semiconductor Technology and Science*, vol. 12, no. 1, pp.53-58, 2012.

[13] S. Lee, "Direct extraction technique for a small-signal MOSFET equivalent circuit with substrate parameters," *Microw. Opt. Technol. Lett*, vol. 39, no. 4, pp. 344-347, 2003.

[14] J.-Y. Kim, M.-K. Choi, and S. Lee, "Accuracy analysis of extraction methods for effective channel length in deep-submicron MOSFETs," *Journal of Semiconductor Technology and Science*, vol. 11, no. 2, pp. 129-132, 2011.

Hyun-Jun Lee was born in Seoul, Korea, in 1986. He received the B.S. degree in electronic engineering in 2012 from the Hankuk University of Foreign Studies, Yongin, Korea, where he is currently working toward the M.S. degree in electronic engineering in the Department of Electronics and Information Engineering. His current research work is focused on RF CMOS modeling and parameter extraction for RF circuit design.

Seonghearn Lee was born in Junjoo, Korea, in 1962. He received the B.E. degree in electronic engineering in 1985 from Korea University, Seoul, Korea, and the M.S. and Ph.D. degrees in electrical engineering from the University of Minnesota, Minneapolis, in 1989 and 1992, respectively. His doctoral dissertation work involved the design, fabrication, and parameter extraction of AlGaAs/GaAs heterojunction bipolar transistors. From 1992 to 1995, he was a Senior Member of the Research Staff with the Semiconductor Technology Division, Electronics and Telecommunications Research Institute, Taejon, Korea, where he worked on the development of polysilicon emitter bipolar transistors and Si/SiGe/Si heterojunction bipolar transistors. Since 1995, he has been with the

Department of Electronic Engineering, Hankuk University of Foreign Studies, Yongin, Korea, where he is currently a Professor. Since 1996, he has carried out research on RF CMOS and bipolar compact modeling and parameter extraction for the RF circuit design in wireless communications applications. Lately, he has successfully developed SPICE model library for SOI RF CMOS Process at the National NanoFab Center, Taejon, Korea. His research interests are in the field of design, modeling, and characterization of silicon and compound semiconductor devices for use in high-frequency integrated circuits. Prof. Lee is a senior member of the IEEE Electron Devices Society and a member of the Institute of Electronics Engineers of Korea. He received the HUFS Excellence in Research Award from the Hankuk University of Foreign Studies, in 2001, 2003, and 2004. He has been listed in *Who's Who in the World* and *Who's Who in Asia*.